



OPEN

## Construction of active-inert core–shell structured nanocrystals for broad range multicolor upconversion luminescence

Mengyao Zhu<sup>1</sup>, Zhenhua Li<sup>2</sup>, Xuecheng Li<sup>1</sup>, Xueru Zhang<sup>2</sup>, Yuxiao Wang<sup>2</sup>, Haoyue Hao<sup>1✉</sup> & Liang Li<sup>1✉</sup>

Rare earth doped up-conversion luminescent nano-materials exhibit abundant emission colors under suitable excitation condition. In this work,  $\text{NaYF}_4:\text{Er}/\text{Ho}@/\text{NaYF}_4$  and  $\text{NaYbF}_4:\text{Tm}@/\text{NaYF}_4$  nanoparticles were synthesized by co-precipitation method. The pure red emission can be realized by the designed  $\text{NaYF}_4:\text{Er}/\text{Ho}@/\text{NaYF}_4$  nanocrystals and the R/Gs reach 23.3 and 25 under excitations of 980 and 1550 nm lasers, respectively. The R/G declines as the power increasing with the emission color changing from red to yellow, which is due to the quick saturation of the energy levels, radiating red emissions. Meanwhile, the emission intensity of  $\text{NaYbF}_4:\text{Tm}@/\text{NaYF}_4$  nanocrystals increases by 58.3 folds after encasing the inert shell  $\text{NaYF}_4$  and the CIE color coordinate reaches (0.1646, 0.0602) under 980 nm laser excitation. Furthermore, broad range multicolor from blue to red and yellow up-conversion emissions is achieved by mixing  $\text{NaYF}_4:\text{Er}/\text{Ho}@/\text{NaYF}_4$  and  $\text{NaYbF}_4:\text{Tm}@/\text{NaYF}_4$  nanocrystals, which could be applied to colorful displaying, security anti-counterfeiting and information coding.

**Keywords** Up-conversion, Core–shell structure, Emission color tuning, Energy transfer

Rare earth ions doped up-conversion luminescent nano-materials, benefiting from the unique 4f energy level of trivalent rare earth ions<sup>1</sup>, have draw extensive attention in many research fields, like bio-imaging<sup>2,3</sup>, solid-state lasers<sup>4,5</sup>, optical temperature sensing<sup>6,7</sup> and anti-counterfeiting<sup>8,9</sup>. Due to the remarkable physical and chemical stability, large anti-Stokes shift, multiple emission span and long emission lifetime, the rare earth ions doped materials show a broad application prospects in colorful displaying<sup>10–20</sup>. In up-conversion luminescent nano-materials,  $\text{Er}^{3+}$  ( $^2\text{H}_{11/2}/^4\text{S}_{3/2} \rightarrow ^4\text{I}_{15/2}; ^4\text{F}_{9/2} \rightarrow ^4\text{I}_{15/2}$ ) and  $\text{Ho}^{3+}$  ( $^5\text{F}_4/^3\text{S}_2 \rightarrow ^5\text{I}_8; ^5\text{F}_5 \rightarrow ^5\text{I}_8$ ) are used to achieve green and red emission colors under infrared light excitation.  $\text{Tm}^{3+}$  ( $^1\text{G}_4 \rightarrow ^3\text{H}_6; ^1\text{G}_4 \rightarrow ^3\text{F}_4$ ) is used to obtain the blue and red emission colors<sup>10,11</sup>. While, the up-conversion emission colors, like green and red emissions radiated from  $\text{Er}^{3+}$ , are accompanied with each other. The single emission from up-conversion phosphor is rare. Therefore, it is important and necessary to obtain a pure emission color, especially red emission color, for colorful displaying. Generally, the pure emission color can be tuned through by selecting proper ratio of co-doping rare ions and engineering local structure<sup>13–17</sup>. Guo et al. reported that the pure green, red and blue emissions are obtained in  $\text{Yb}^{3+}/\text{Ln}^{3+}$  (Ln = Er, Ho, Tm) co-doped  $\text{Gd}_2\text{O}_3$  up-conversion phosphors by adjusting the doping concentration of  $\text{Er}^{3+}$ ,  $\text{Ho}^{3+}$  and  $\text{Tm}^{3+}$ , which is attributed to the strengthened cross relaxation processes<sup>14</sup>. To obtain broader range emission colors, the core–shell structured nano-materials are rational design in the past few years<sup>11,18–22</sup>. Jang et al. reported that the emission colors from heavily doped  $\text{NaErF}_4:\text{Tm}$ -based core@ multi-shell nano-materials were fine tuned through changing the excitation laser from 980 to 808 and 1550 nm and the full-color emissions, including green, red and blue, were achieved via combination effects of elemental migration and photon blocking<sup>19</sup>. These researches indicate that the wide range emission color could be possibly achieved via rational designing core–shell structured nano-materials and tailoring the up-conversion processes. What's more, other methods, like combining localized surface plasmon resonance (LSPR) and modifying quantum dots or dyes were also utilized to tune the emission color<sup>23–26</sup>.

<sup>1</sup>School of Physics and Optoelectronic Engineering, Shandong University of Technology, Zibo 255000, People's Republic of China. <sup>2</sup>Department of Physics, Harbin Institute of Technology, Harbin 150001, People's Republic of China. ✉email: haohao\_yue@163.com; liangli@sdut.edu.cn

In this work, the pure red and blue emissions are realized through the simple double-layer structured  $\text{NaYF}_4:\text{Er}/\text{Ho}@\text{NaYF}_4$  and  $\text{NaYbF}_4:\text{Tm}@\text{NaYF}_4$  nanocrystals under excitation of 980 nm laser and the color can also be fine tuned from blue to red via tuning the mass ratio of the two samples, with the corresponding CIE chromatic coordinates changing from (0.1599, 0.0388) to (0.7010, 0.2813). The red to green ratios (R/Gs) reach 23.3 and 25 of  $\text{NaYF}_4:\text{Er}/\text{Ho}@\text{NaYF}_4$  nanocrystals under excitation of 980 and 1550 nm lasers, respectively, which is originated to the energy transfer processes between  $\text{Er}^{3+}$  and  $\text{Ho}^{3+}$ .

## Experimental

### Synthesis of $\text{NaYF}_4:\text{Er}/\text{Ho}@\text{NaYF}_4$ and $\text{NaYbF}_4:\text{Tm}@\text{NaYF}_4$ core-shell structured nanocrystals

#### Synthesis of $\text{NaYF}_4:\text{Er}/\text{Ho}$ nanocrystals

$\text{NaYF}_4:\text{Er}/\text{Ho}$  up-conversion nanocrystals were prepared through co-precipitation of the lanthanide chloride with oleic acid and 1-octadecene<sup>27</sup>, where  $\text{YCl}_3 \cdot 6\text{H}_2\text{O}$  (99.9%),  $\text{ErCl}_3 \cdot 6\text{H}_2\text{O}$  (99.9%) and  $\text{HoCl}_3 \cdot 6\text{H}_2\text{O}$  (99.9%) were used as original materials. 1 mmol  $\text{LnCl}_3 \cdot 6\text{H}_2\text{O}$  ( $\text{Ln} = 86.3\% \text{Y}, 13.5\% \text{Er}, 0.2\% \text{Ho}$ ), 6 ml of oleic acid and 15 ml of 1-octadecene were added into a 50 mL three-necked flask simultaneously. Heated the mixture to 150 °C and kept it at this temperature for 40 min. After cooling to 50 °C, a methanol mixture of 2.5 mmol NaOH and 4 mmol  $\text{NH}_4\text{F}$  was added to the three-necked flask and kept the reaction at this temperature for 40 min. Subsequently, the mixture was heated to 120 °C for 20 min to eliminate remaining water and methanol. Finally, the temperature of the mixture was increased to 310 °C for 1 h. The obtained nanocrystals were dispersed in 10 ml cyclohexane as the precursor solution of core-shell structure after washing with cyclohexane and ethanol in a ratio of 1:3.

#### Synthesis of $\text{NaYF}_4:\text{Er}/\text{Ho}@\text{NaYF}_4$ nanocrystals

$\text{NaYF}_4:\text{Er}/\text{Ho}@\text{NaYF}_4$  nanocrystals were prepared through the similar procedure. 1 mmol  $\text{YCl}_3 \cdot 6\text{H}_2\text{O}$  were used as original materials. The methanol mixture of 2.5 mmol NaOH, 4 mmol  $\text{NH}_4\text{F}$  and the precursor solution ( $\text{NaYF}_4:\text{Er}/\text{Ho}$ ) were added to the three-necked flask simultaneously. The obtained nanocrystals were washed and dried at 60 °C in air for 12 h for up-conversion luminescence tested.

#### Synthesis of $\text{NaYbF}_4:\text{Tm}$ and $\text{NaYbF}_4:\text{Tm}@\text{NaYF}_4$ nanocrystals

$\text{NaYbF}_4:0.5\text{Tm}$  and  $\text{NaYbF}_4:0.5\text{Tm}@\text{NaYF}_4$  nanocrystals were prepared through the above procedure. Only the rare earth ions and the doped ratio differed from the previous samples.

## Measurements and characterization

The X-ray powder diffraction (XRD) patterns were recorded using a Bruker D8 diffractometer to investigate the phase purity and phase structure of the samples. The transmission electron microscope (TEM) images were recorded by a Talos F200X G2 field emission electron microscope to investigate the morphologies of the samples. The 980 nm laser (EC31439), using to excite the sample, was purchased from Changchun New Industries Opto-electronics Tech Co., Ltd. The 1550 nm laser (BTW DS2-21312110), using to excite the sample, was purchased from Beijing Kipling Photoelectric technology Co., Ltd. The up-conversion emission spectra of the samples were measured through the fiber optic spectrometer purchased from Chen Xu instrument Co., Ltd (Type: ST4000). The time-dependent emission profiles of the samples were recorded using iHR550 grating spectrometer with a DSO5032A Digital Storage Oscilloscope.

## Results and discussion

### Structure and morphological characterization

XRD patterns of all samples are illustrated in Fig. 1a. Compared with the two kinds of standard hexagonal phase  $\text{NaYF}_4$  (JCPDS No.16-0334) and  $\text{NaYbF}_4$  (JCPDS No.27-1427),  $\text{NaYF}_4:\text{Er}/\text{Ho}$  and  $\text{NaYF}_4:\text{Er}/\text{Ho}@\text{NaYF}_4$

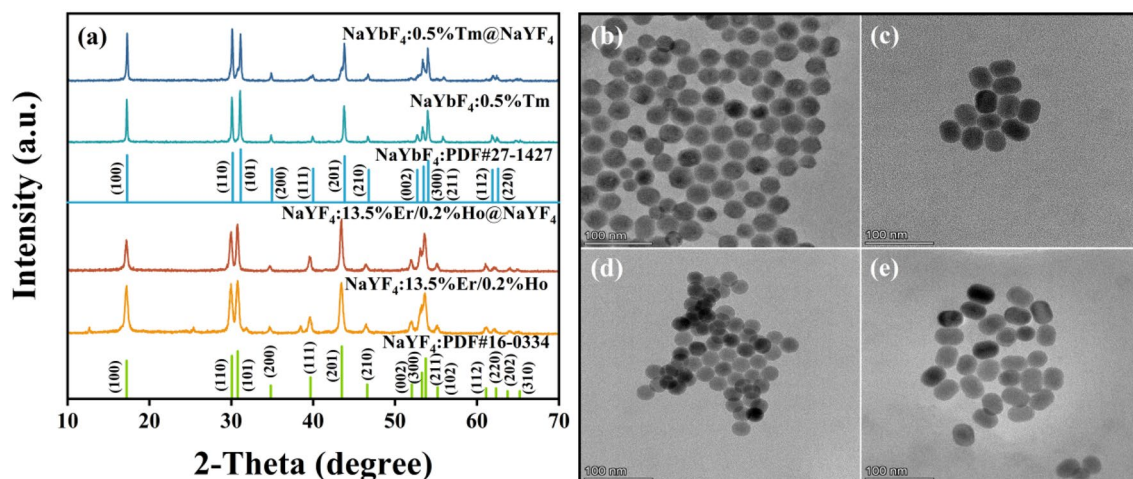


**Figure 1.** (a) XRD patterns  $\text{NaYF}_4:\text{Er}/\text{Ho}$ ,  $\text{NaYF}_4:\text{Er}/\text{Ho}@\text{NaYF}_4$ ,  $\text{NaYbF}_4:\text{Tm}$  and  $\text{NaYbF}_4:\text{Tm}@\text{NaYF}_4$ ; TEM images of (b)  $\text{NaYbF}_4:\text{Tm}$  (c)  $\text{NaYbF}_4:\text{Tm}@\text{NaYF}_4$  (d)  $\text{NaYF}_4:\text{Er}/\text{Ho}$  (e)  $\text{NaYF}_4:\text{Er}/\text{Ho}@\text{NaYF}_4$  nanocrystals.

nanocrystals are pure hexagonal phase NaYF<sub>4</sub>. NaYbF<sub>4</sub>:Tm and NaYbF<sub>4</sub>:Tm@NaYF<sub>4</sub> nanocrystals are pure hexagonal phase NaYbF<sub>4</sub>. Figure 1b–e show TEM images of NaYbF<sub>4</sub>:Tm, NaYbF<sub>4</sub>:Tm@NaYF<sub>4</sub>, NaYF<sub>4</sub>:Er/Ho and NaYF<sub>4</sub>:Er/Ho@NaYF<sub>4</sub> nanocrystals, respectively. As shown in Fig. 1b, the obtained NaYbF<sub>4</sub>:Tm nanocrystals is composed of monodisperse sphere and the average diameter is ~28.5 nm. After coating by inert shell NaYF<sub>4</sub>, the NaYbF<sub>4</sub>:Tm@NaYF<sub>4</sub> nanocrystals are prepared, where the nanospheres become ellipsoid and the average size increases to ~41.1 × 31.9 nm. As revealed in Fig. 1d, the average size of single core NaYF<sub>4</sub>:Er/Ho nanocrystals is ~26.1 nm and the nanocrystals distribute homogeneously. The morphology of NaYF<sub>4</sub>:Er/Ho@NaYF<sub>4</sub> nanocrystals is similar to NaYbF<sub>4</sub>:Tm@NaYF<sub>4</sub> nanocrystals and the average size is ~39.9 × 30.3 nm. The size distribution diagrams of these nanocrystals are shown in Fig. S1.

### Up-conversion luminescent properties

#### Up-conversion emission spectra and emission color of NaYF<sub>4</sub>:Er/Ho, NaYF<sub>4</sub>:Er/Ho@NaYF<sub>4</sub> nanocrystals

The Er<sup>3+</sup> and Ho<sup>3+</sup> co-doping NaYF<sub>4</sub> nanocrystals are responsive to the excitation wavelengths of 980 and 1550 nm. Figure 2a shows the up-conversion emission spectra of the NaYF<sub>4</sub>:Er/Ho nanocrystals under 980 nm laser excitation (0.35W, 0.45W, 1.05W), where the emission spectra were normalized at 654 nm. The typical emission bands of Er<sup>3+</sup> located at 524, 540 and 655 nm are observed, which corresponding to the radiated transitions of <sup>2</sup>H<sub>11/2</sub> → <sup>4</sup>I<sub>15/2</sub>, <sup>4</sup>S<sub>3/2</sub> → <sup>4</sup>I<sub>15/2</sub> and <sup>4</sup>F<sub>9/2</sub> → <sup>4</sup>I<sub>15/2</sub> respectively. What more, comparing with the emission spectrum of NaYF<sub>4</sub>:Er (shown in Fig. S2), part of the emissions from the NaYF<sub>4</sub>:Er/Ho nanocrystals belong to the green-emitted <sup>5</sup>F<sub>4</sub>, <sup>5</sup>S<sub>2</sub> → <sup>5</sup>I<sub>8</sub> transitions and the red-emitted <sup>5</sup>F<sub>4</sub> → <sup>5</sup>I<sub>8</sub> transition in Ho<sup>3+</sup>. The R/G ratio are 18.7, 7.6 and 3.6 as the power of 980 nm laser changes to 0.35, 0.45 and 1.05, respectively. Comparing to Er<sup>3+</sup> doped NaYF<sub>4</sub> nanocrystals, the value of R/G increases obviously in Er<sup>3+</sup> and Ho<sup>3+</sup> co-doped NaYF<sub>4</sub> nanocrystals, which is due to the new energy transfer processes between Er<sup>3+</sup> and Ho<sup>3+</sup> ions<sup>28</sup>. In the Er<sup>3+</sup>/Ho<sup>3+</sup> co-doped system, Er<sup>3+</sup> ions can absorb the energy of 980 nm laser as a kind of sensitizer and transfer part of energy to the co-doped Ho<sup>3+</sup>. Based on the well energy level overlap between the Er<sup>3+</sup> and Ho<sup>3+</sup>, the energy transfer ET1 (Er<sup>3+</sup>: <sup>4</sup>F<sub>9/2</sub> → Ho<sup>3+</sup>: <sup>5</sup>F<sub>5</sub>), ET2 (Er<sup>3+</sup>: <sup>2</sup>H<sub>11/2</sub>/<sup>4</sup>S<sub>3/2</sub> → Ho<sup>3+</sup>: <sup>5</sup>F<sub>4</sub>/<sup>5</sup>S<sub>2</sub>) and the ground state absorption (Er<sup>3+</sup>: <sup>4</sup>I<sub>15/2</sub> → <sup>4</sup>I<sub>11/2</sub>), excited state absorption (Er<sup>3+</sup>: <sup>4</sup>I<sub>11/2</sub> → <sup>2</sup>H<sub>11/2</sub>/<sup>4</sup>S<sub>3/2</sub> and <sup>4</sup>I<sub>13/2</sub> → <sup>4</sup>F<sub>9/2</sub>) are shown in Fig. 2b. As shown in Fig. 2c, the R/G decreases from 18.7 to 3.6 with the rise of power. The reason for the decrease could be explanation as follows. The R/G value mainly depends on the depletion of the energy level <sup>4</sup>I<sub>11/2</sub> (Er<sup>3+</sup>). There are two channels for the depletion of <sup>4</sup>I<sub>11/2</sub>, including excited state absorption <sup>4</sup>I<sub>11/2</sub> → <sup>4</sup>F<sub>7/2</sub> and non-radiative relaxation <sup>4</sup>I<sub>11/2</sub> → I<sub>13/2</sub>. When the pump power is very small, the up-conversion process of <sup>4</sup>I<sub>11/2</sub> mainly contributes to the population of the energy level I<sub>13/2</sub>

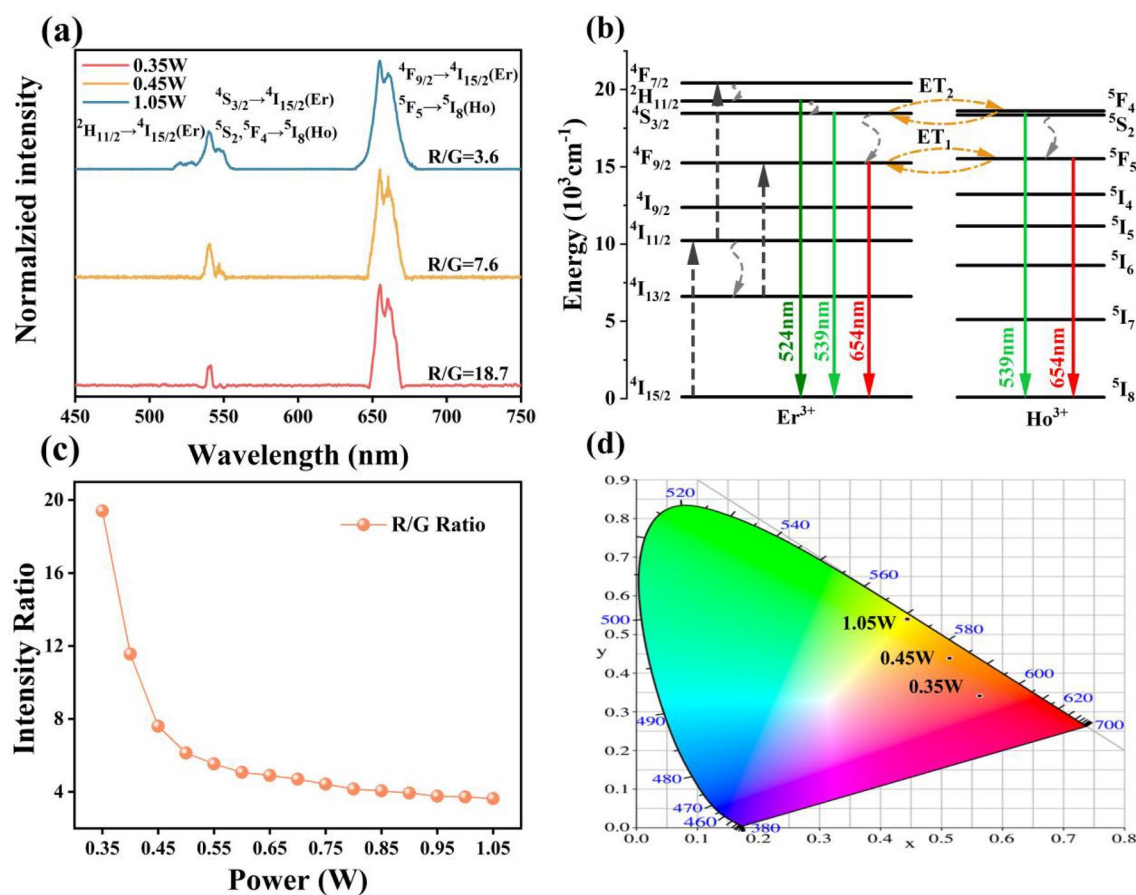


**Figure 2.** (a) Normalized emission spectra of NaYF<sub>4</sub>:Er/Ho nanocrystals under 980 nm laser excitation; (b) The proposed up-conversion and energy transfer processes; (c) R/G variation and (d) the corresponding CIE chromatic coordinates at different powers.

due to the non-radiative relaxation and then populate the red light-emitting level through excited state absorption  $I_{13/2} \rightarrow {}^4F_{9/2}$ . With the increase of pumping power, a considerable part of the electrons on  ${}^4I_{11/2}$  will populate the green light-emitting level through the up-conversion process, which in turn reduces the proportion of red light-emitting level<sup>29,30</sup>. As shown in Fig. 2d, the corresponding CIE chromatic coordinate changes from red to yellow as the power increases and the detail CIE chromatic coordinates are displayed in Table S1.

Figure 3a shows the emission intensity enhancement factor of  $\text{NaYF}_4:\text{Er}/\text{Ho}@/\text{NaYF}_4$  nanocrystals. The enhancement factors of green (539 nm) and red (654 nm) emissions show a slow downward trend as laser power increases. And the enhancement factor of green emissions decreases from 1.29 to 1.18. The enhancement factor of red emission decreases from 2.33 to 1.88. The enhancement factor of the red declines faster with increasing power than that of the green emissions. The emission enhancement is due to the suppression of surface quenching, as shown in Fig. 3b. The emission lifetimes of green and red emissions change longer as the  $\text{NaYF}_4$  shell are coated (as shown in Fig. S3), which confirms the decline of surface quenching<sup>31</sup>. And the more obvious enhancement of red emission might be originated to the increased ET1 process. It is worth to mention that the R/G decreases from 23.3 to 5.8 with the increasing of power from 0.35 to 1.05 W (as shown in Fig. 3c). As a result, comparing to  $\text{NaYF}_4:\text{Er}/\text{Ho}$  nanocrystals, the corresponding CIE chromatic coordinate changes to deep red region (as shown in Fig. 3d and Table S2).

To investigate the non-steady up-conversion processes, the up-conversion emission spectra of  $\text{NaYF}_4:\text{Er}/\text{Ho}@/\text{NaYF}_4$  at different pulse widths from 500 to 1300  $\mu\text{s}$  were tested (the pulse frequency was fixed at 600 Hz). As shown in Fig. 4a, the green emissions are weak and become obviously as the pulse width enlarges. And the value of R/G ratio decreases from 9.3 to 6.5 with the pulse duration times increasing from 500 to 1300  $\mu\text{s}$ , as shown in Fig. 4b. This phenomenon is different to the tendency of other rare ions doped materials, like  $\text{Ho}(\text{Er})/\text{Yb}$ , where the R/G rises as the pulse widths increase<sup>32,33</sup>. To explain the reason why the R/G declines with pulse width rise, we investigated the non-steady state behavior of the sample under 980 nm laser excitation. As shown in Fig. 4c, the intensity of green and red emissions rise slowly under excitation. And the rise time is longer than the nanocrystals without  $\text{NaYF}_4$  shell (as shown in Fig. S4), indicating that the  $\text{NaYF}_4$  shell intensifies the ET1 and ET2. The similar rise tendency of green and red emissions, unlike the shorter rise time of green emissions in other reports<sup>32–34</sup>, make the different R/G change tendency with pulse width increasing. The reason of the slower rise time of this sample is that the ET1, ET2, back-ET1 (BET1), back-ET2 (BET2) and non-radiative relaxation processes, as shown in Fig. 3b, repopulate the energy levels of  ${}^4F_{9/2}$ ,  ${}^2H_{11/2}$ ,  ${}^4S_{3/2}$ ,  ${}^5F_5$ ,  ${}^5F_4/{}^5S_2$ .

Upon changing the excitation wavelength to 1550 nm, the emission spectra of  $\text{NaYF}_4:\text{Er}/\text{Ho}@/\text{NaYF}_4$  nanocrystals are detected under 1550 nm laser. As shown in Fig. 4d, the value of R/G reaches 25 under low power

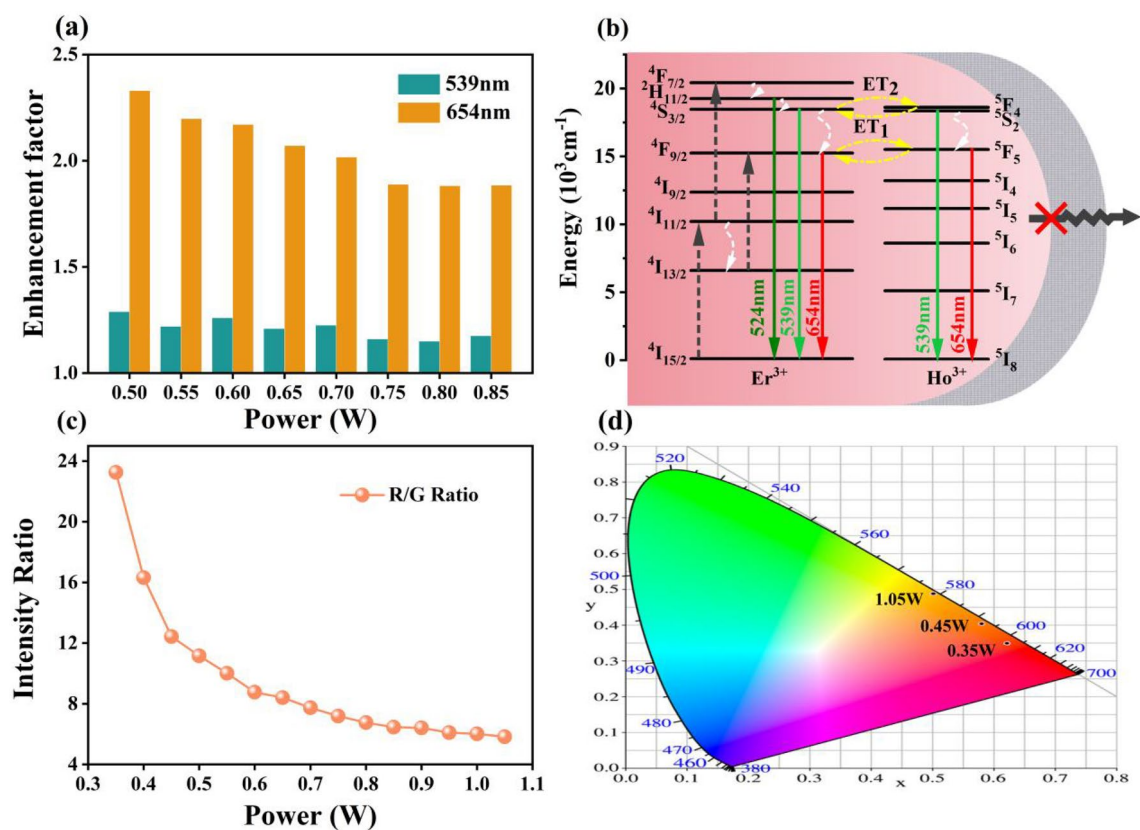


**Figure 3.** (a) The enhancement factor (c) dependence of R/G and (d) the corresponding CIE chromatic coordinates of  $\text{NaYF}_4:\text{Er}/\text{Ho}@/\text{NaYF}_4$  nanocrystals under 980 nm laser excitation with different powers; (b) The proposed up-conversion processes and surface quenching.



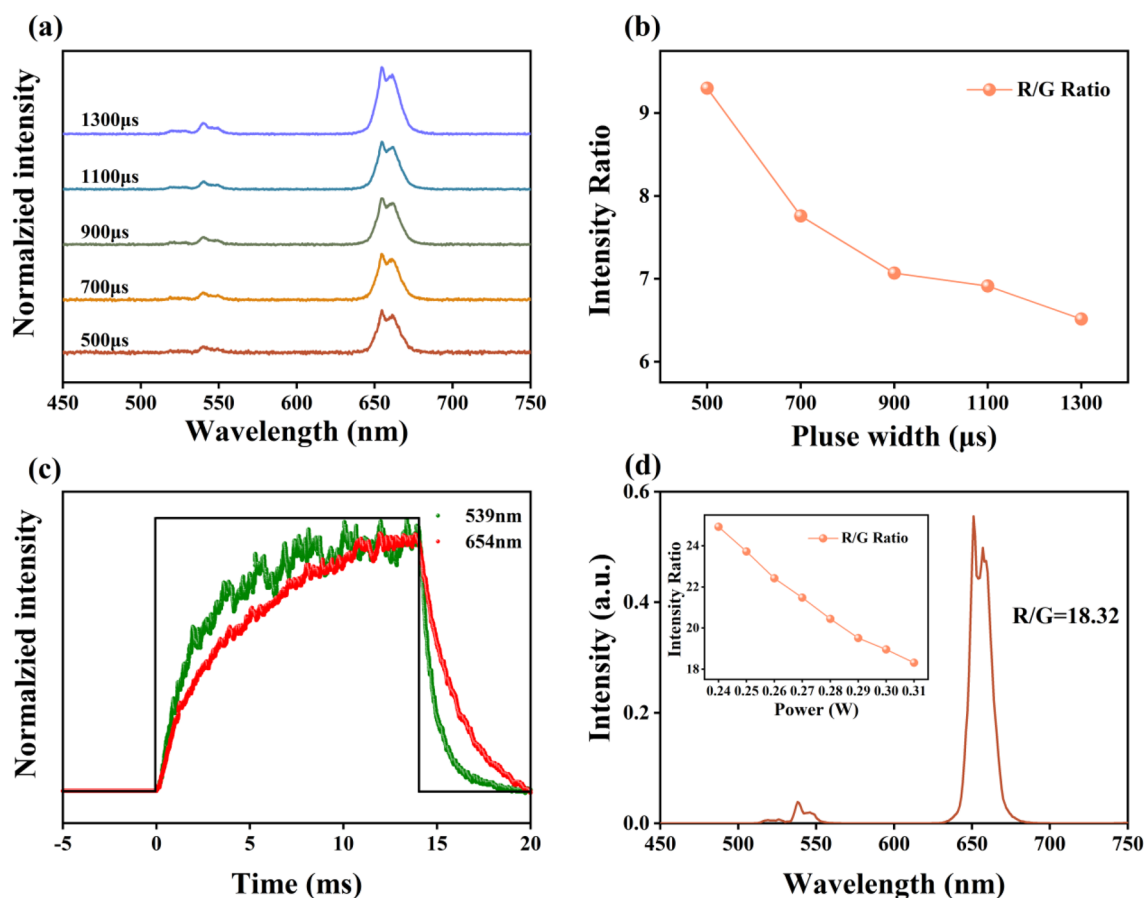


**Figure 4.** (a) Normalized emission spectra and (b) the R/G of  $\text{NaYF}_4\text{:Er/Ho@NaYF}_4$  nanocrystals under 980 nm laser excitation at different pulse width; (c) Time-dependent green and red emission profiles of  $\text{NaYF}_4\text{:Er/Ho@NaYF}_4$  nanocrystals; (d) The up-conversion emission spectra of  $\text{NaYF}_4\text{:Er/Ho@NaYF}_4$  nanocrystals under 1550 nm laser excitation, the insert show the R/G with different excitation powers.

excitation and show the similarity decrease tendency as laser power increases. Comparing with sample under 980 nm laser excitation, the larger value of R/G is obtained under 1550 nm laser excitation. This phenomenon can be interpreted with the original populations of energy levels of  $\text{Er}^{3+}$ :  $^4\text{F}_{9/2}$ ,  $^2\text{H}_{11/2}$ ,  $^4\text{S}_{3/2}$ , which can be deduced from the up-conversion emission spectrum of  $\text{NaYF}_4\text{:Er}$  under 1550 nm laser excitation (as shown in Fig. S5). The large R/G value indicates that the  $\text{NaYF}_4\text{:Er/Ho@NaYF}_4$  nanocrystals can be used as red phosphors under 980 and 1550 nm laser excitation.

#### Up-conversion emission spectra and emission color of $\text{NaYbF}_4\text{:Tm}$ and $\text{NaYbF}_4\text{:Tm@NaYF}_4$ nanocrystals

To obtain the pure blue phosphors, the bare core  $\text{NaYbF}_4\text{:Tm}$  and core-shell  $\text{NaYbF}_4\text{:Tm@NaYF}_4$  structured nanocrystals were prepared. It can be observed in Fig. 5a, after coating the inert shell with  $\text{NaYbF}_4\text{:Tm}$ , the emission intensity of  $\text{NaYbF}_4\text{:Tm@NaYF}_4$  increases by 58.3 fold. It should be mentioned that the  $\text{NaYF}_4$  shell plays an important role in inhibiting surface quenching and increasing emission intensity. The intense blue emissions at 450 and 472 nm makes the emission color display pure blue, as shown in the insert of Fig. 5a (the detail CIE chromatic coordinates are displayed in Table S3). The relevant up-conversion processes are displayed in Fig. 5b. The efficient energy transferred from  $\text{Yb}^{3+}$  can be used to populated the energy levels of  $^1\text{D}_2$ ,  $^1\text{G}_4$  and then radiated intense blue emissions. What's more, the emission color almost unchanges with the increasing of laser power, as shown in Fig. S6, which provides the possibility for the mixed materials to regulate emission color.

#### Broad bange upconversion emission spectra and emission color

In order to realize the broad domain multicolor up-conversion luminescence, these two types of distinct phosphors,  $\text{NaYbF}_4\text{:Tm@NaYF}_4$  and  $\text{NaYF}_4\text{:Er/Ho@NaYF}_4$  nanocrystals, were dissolve in alcohol and grind in accordance with fixed mass ratio: ① only  $\text{NaYbF}_4\text{:Tm@NaYF}_4$  nanocrystals, ② 1:10, ③ 1:5, ④ 1:2 and ⑤ only  $\text{NaYF}_4\text{:Er/Ho@NaYF}_4$  nanocrystals. The emission spectra of the mixed samples are shown in the Fig. 6a, and the corresponding CIE chromatic coordinates are presented in Fig. 6b. As expected, Fig. 6b shows a wide range of color diversity from blue to red, including blue (0.1613, 0.0421), purple (0.2604, 0.0872), magenta (0.3722, 0.1489), crimson (0.5506, 0.2474) and red (0.6700, 0.3202). We also investigated the luminescence properties of these samples under excitation with different 980 nm laser power, as shown in Fig. S7. As the power increases, the CIE chromatic coordinates go to the red and green region (the detail CIE chromatic coordinates are displayed

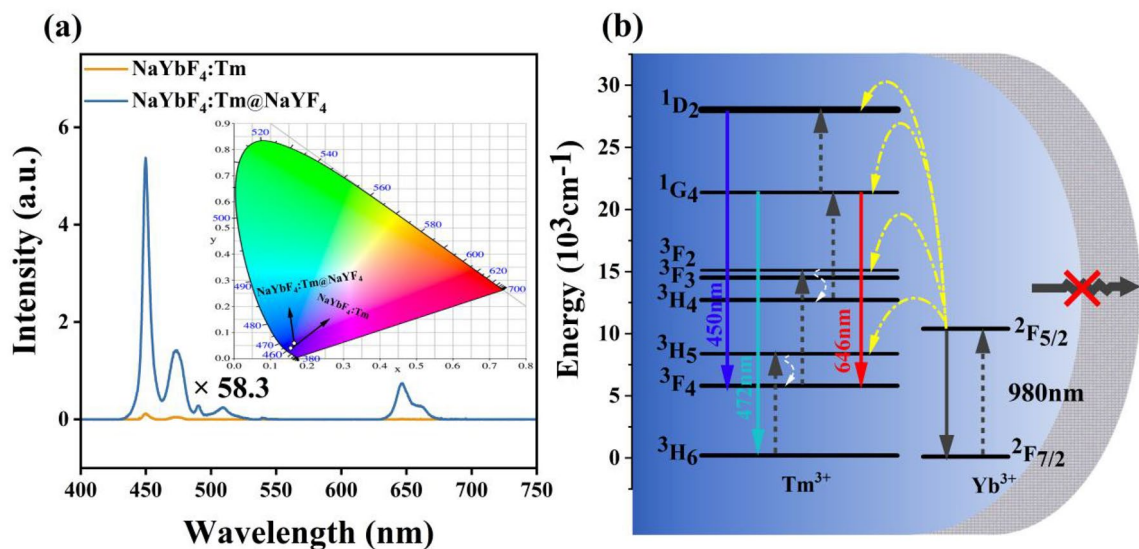


**Figure 5.** (a) The up-conversion emission spectra of  $\text{NaYbF}_4:\text{Tm}$  and  $\text{NaYbF}_4:\text{Tm}@ \text{NaYF}_4$  nanocrystals, the insert show the corresponding CIE chromatic coordinates; (b) The proposed up-conversion luminescent mechanism.

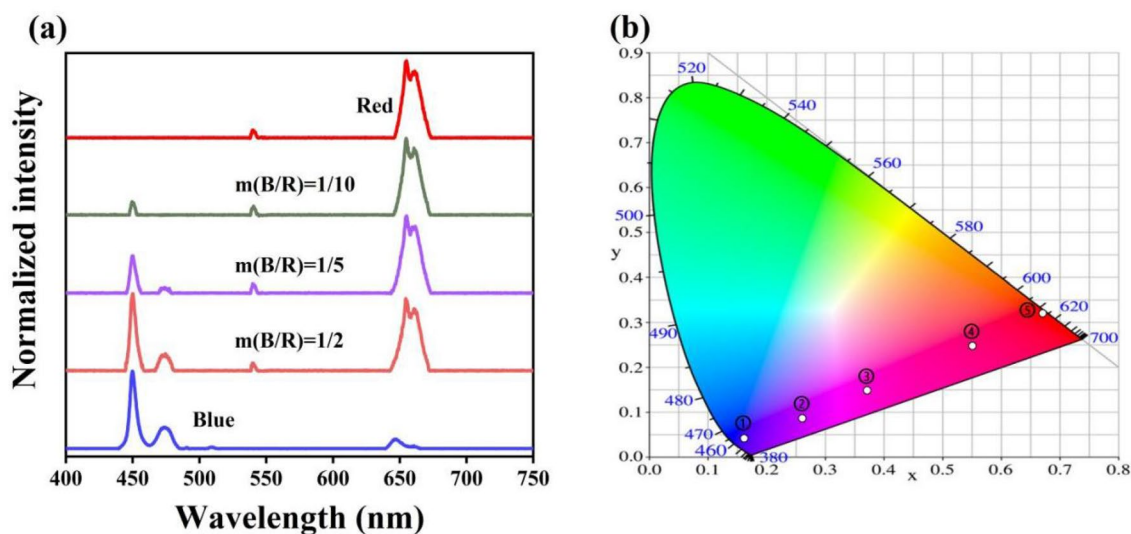


**Figure 6.** (a) Normalized emission spectra (b) the corresponding CIE chromatic coordinates of samples with fixed mass ratio under 980 nm laser excitation.

in Table S4), which eventually occupy over one-third of the entire chromaticity diagram. This result indicates that the composites may find applications in colorful displaying and anti-counterfeiting.

## Conclusions

In summary, we designed double-layer core-shell structure to investigate the effect of excitation condition on up-conversion emission spectra and emission color. The pure red emission can be realized by the designed  $\text{NaYF}_4:\text{Er}/\text{Ho}@ \text{NaYF}_4$  nanocrystals under 980 or 1550 nm laser excitation. And the R/G declines as the power of 980 nm laser increases, with the emission color changing from red to yellow, which can be interpreted by the quick saturation of the energy levels, radiating red emissions. Because of the ET, BET and non-radiative relaxation processes among  $\text{Ho}^{3+}$  and  $\text{Er}^{3+}$ , the R/G also decreases as the pulse width rises. Meanwhile, the up-conversion luminescence of  $\text{NaYbF}_4:\text{Tm}@ \text{NaYF}_4$  phosphors under 980 nm laser excitation were also studied. After encasing the inert shell  $\text{NaYF}_4$ , the emission intensity from  $\text{NaYbF}_4:\text{Tm}@ \text{NaYF}_4$  nanocrystals increases by 58.3 folds. A wide range emission colors from blue to red, including blue, purple, magenta, crimson and red are realized through tuning the mass ratio of two samples. As the power increasing, the CIE chromatic coordinates go to the red and green region and eventually occupy over one-third of the entire chromaticity diagram. These results indicate the potential applications of these materials in various fields, including colorful displaying, security anti-counterfeiting and information coding.

## Data availability

The datasets used and/or analysed during the current study available from the corresponding author on reasonable request.

Received: 5 February 2024; Accepted: 19 March 2024

Published online: 26 March 2024

## References

- Zheng, B. Z. *et al.* Rare-earth doping in nanostructured inorganic materials. *Chem. Rev.* **122**(6), 5519–5603 (2022).
- Zhang, K. K. *et al.* Nanodiamonds conjugated upconversion nanoparticles for bio-imaging and drug delivery. *J. Colloid Interface Sci.* **537**, 316–324 (2019).
- Zhou, J., Liu, Z. & Li, F. Y. Upconversion nanophosphors for small-animal imaging. *Chem. Soc. Rev.* **41**(3), 1323–1349 (2012).
- Heumann, E. *et al.* Semiconductor-laser-pumped high-power upconversion laser. *Appl. Phys. Lett.* **88**(6), 061109 (2006).
- Kim, J. W., Mackenzie, J. I. & Clarkson, W. A. Influence of energy-transfer-upconversion on threshold pump power in quasi-three-level solid-state lasers. *Opt. Express* **17**(14), 11935–11943 (2009).
- Runowski, M. *et al.* Upconverting lanthanide fluoride core@shell nanorods for luminescent thermometry in the first and second biological windows:  $\beta$ -NaYF<sub>4</sub>:Yb<sup>3+</sup>-Er<sup>3+</sup>@ SiO<sub>2</sub> temperature sensor. *ACS Appl. Mater. Interfaces* **11**(14), 13389–13396 (2019).
- Du, P., Luo, L. H., Park, H. K. & Yu, J. Citric-assisted sol-gel based Er<sup>3+</sup>/Yb<sup>3+</sup>-codoped Na<sub>0.5</sub>Gd<sub>0.5</sub>MoO<sub>4</sub>: A novel highly-efficient infrared-to-visible upconversion material for optical temperature sensors and optical heaters. *Chem. Eng. J.* **306**, 840–848 (2016).
- Huang, J. *et al.* Cross relaxation enables spatiotemporal color-switchable upconversion in a single sandwich nanoparticle for information security. *Adv. Mater.* <https://doi.org/10.1002/adma.202310524> (2023).
- Liu, X. *et al.* Binary temporal upconversion codes of Mn<sup>2+</sup>-activated nanoparticles for multilevel anti-counterfeiting. *Nat. Commun.* **8**(1), 899 (2017).
- Ray, S. K., Joshi, B., Ramani, S., Park, S. & Hur, J. Multicolor and white light upconversion luminescence in  $\alpha$ -NiMoO<sub>4</sub>: Yb<sup>3+</sup>/Ln<sup>3+</sup> (Ln=Tm, Ho, Tm/Ho) nanoparticles. *J. Alloy Compd.* **892**, 162101 (2022).
- Hong, A., Kyhm, J. H., Kang, G. & Jang, H. Orthogonal R/G/B upconversion luminescence-based full-color tunable upconversion nanophosphors for transparent displays. *Nano Lett.* **21**(11), 4838–4844 (2021).
- Liu, R. *et al.* ErF<sub>3</sub> microcrystals controllably deposited in perfluoride glass for upconversion red emission. *Opt. Lett.* **48**(24), 6432–6435 (2023).
- Hao, H., Zhang, X., Wang, Y. & Li, L. Color modulation and temperature sensing investigation of Gd<sub>2</sub>O<sub>3</sub>:1mol%Er<sup>3+</sup>,1mol%Yb<sup>3+</sup> phosphors under different excitation condition. *J. Lumin.* **215**, 116556 (2019).
- Zhao, X., Suo, H., Zhang, Z. & Guo, C. Spectral pure RGB up-conversion emissions in self-assembled Gd<sub>2</sub>O<sub>3</sub>: Yb<sup>3+</sup>, Er<sup>3+</sup>/Ho<sup>3+</sup>/Tm<sup>3+</sup> 3D hierarchical architectures. *Ceram. Int.* **44**(3), 2911–2918 (2018).
- Wang, M. *et al.* Pure-green upconversion emission and high-sensitivity optical thermometry of Er<sup>3+</sup>-doped stoichiometric NaYb(MoO<sub>4</sub>)<sub>2</sub>. *Ceram. Int.* **49**(23), 37661–37669 (2023).
- Fu, H. *et al.* A general strategy for tailoring upconversion luminescence in lanthanide-doped inorganic nanocrystals through local structure engineering. *Nanoscale* **10**(19), 9353–9359 (2018).
- Li, H. *et al.* Sc<sup>3+</sup>-induced morphology, phase structure, and upconversion luminescence evolution of YF<sub>3</sub>:Yb/Er nanocrystals. *J. Mater. Chem. C* **5**(26), 6450–6456 (2017).
- Huang, K. *et al.* Orthogonal trichromatic upconversion with high color purity in core-shell nanoparticles for a full-color display. *Angew. Chem.* **135**(14), e202218491 (2023).
- Mun, K. *et al.* Elemental-migration-assisted full-color-tunable upconversion nanoparticles for video-rate three-dimensional volumetric displays. *Nano Lett.* **23**(7), 3014–3022 (2023).
- Xie, Z. *et al.* Rationally-designed core-shell structure with double-plasmon effect for efficient and tunable upconversion luminescence emission. *Appl. Surf. Sci.* **643**, 158726 (2024).
- Yuan, X. *et al.* Triple-mode upconversion emission for dynamic multicolor luminescent anti-counterfeiting. *J. Colloid Interface Sci.* **2023**(641), 961–971 (2023).
- Li, L., Xing, F., Zhang, X., Hao, H. & Wang, Y. Emission enhancement and color modulation of Tm(Ho)/Yb codoped Gd<sub>2</sub>(MoO<sub>4</sub>)<sub>3</sub> thin films via the use of multilayered structure. *J. Rare Earth* **39**(7), 765–771 (2021).
- Liu, J. *et al.* Construction of a novel pitaya-like Cs<sub>x</sub>WO<sub>3</sub>@NaYF<sub>4</sub>:Yb, Er particles with simultaneous colour tuning and upconversion luminescence enhancement. *J. Alloy Compd.* **854**, 157139 (2021).
- Qin, X. *et al.* Surface plasmon-photon coupling in lanthanide-doped nanoparticles. *J. Phys. Chem. Lett.* **12**(5), 1520–1541 (2021).
- Du, K. *et al.* Embellishment of upconversion nanoparticles with ultrasmall perovskite quantum dots for full-color tunable, dual-modal luminescence anticounterfeiting. *Adv. Opt. Mater.* **9**(21), 2100814 (2021).
- Cheng, X., Tu, D., Zheng, W. & Chen, X. Energy transfer designing in lanthanide-doped upconversion nanoparticles. *Chem. Commun.* **56**(96), 15118–15132 (2020).
- Wang, F., Deng, R. & Liu, X. Preparation of core-shell NaGdF<sub>4</sub> nanoparticles doped with luminescent lanthanide ions to be used as upconversion-based probes. *Nat. Protoc.* **9**(7), 1634–1644 (2014).
- Cheng, X. *et al.* Design for brighter photon upconversion emissions via energy level overlap of lanthanide ions. *ACS Nano* **12**(11), 10992–10999 (2018).
- Zhou, Z., Zhu, B., Chen, K. & Pang, T. Highly sensitive response of luminescence chromaticity to laser power in Lu<sub>2</sub>Mo<sub>4</sub>O<sub>15</sub>:Yb<sup>3+</sup>/Ho<sup>3+</sup> upconverting materials. *Dalton Trans.* **52**(45), 16732–16736 (2023).
- Pang, T., Jian, R., Mao, J. & Guo, H. Improved response of upconversion luminescence color to pump power through the coupling of Er<sup>3+</sup> and Tm<sup>3+</sup>. *J. Phys. Chem. C* **126**(3), 1481–1488 (2022).
- Cheng, X. *et al.* Er<sup>3+</sup> sensitized photon upconversion nanocrystals. *Adv. Funct. Mater.* **28**, 1800208 (2018).
- Huang, J., An, Z., Yan, L. & Zhou, B. Engineering orthogonal upconversion through selective excitation in a single nanoparticle. *Adv. Funct. Mater.* **33**, 2212037 (2023).
- Deng, R. *et al.* Temporal full-colour tuning through non-steady-state upconversion. *Nat. Nanotechnol.* **10**, 237–242 (2015).
- Lei, B. *et al.* Co-doping of Ho-Yb ion pairs modulating the up-conversion luminescence properties of fluoride phosphors under 1550 nm excitation. *Dalton Trans.* **52**(33), 11489–11502 (2023).

## Acknowledgements

The work was financially supported by the National Natural Science Foundation of China (Grant No. 12004217).

### Author contributions

Mengyao Zhu: Writing—Original Draft, Visualization and Investigation. Zhenhua Li: Formal analysis. Xuecheng Li: Data Curation. Xueru Zhang: Software. Yuxiao Wang: Formal analysis. Haoyue Hao: Writing-Reviewing and Editing, Project administration. Liang Li: Supervision and Funding acquisition.

### Competing interests

The authors declare no competing interests.

### Additional information

**Supplementary Information** The online version contains supplementary material available at <https://doi.org/10.1038/s41598-024-57523-y>.

**Correspondence** and requests for materials should be addressed to H.H. or L.L.

**Reprints and permissions information** is available at [www.nature.com/reprints](http://www.nature.com/reprints).

**Publisher's note** Springer Nature remains neutral with regard to jurisdictional claims in published maps and institutional affiliations.



**Open Access** This article is licensed under a Creative Commons Attribution 4.0 International License, which permits use, sharing, adaptation, distribution and reproduction in any medium or format, as long as you give appropriate credit to the original author(s) and the source, provide a link to the Creative Commons licence, and indicate if changes were made. The images or other third party material in this article are included in the article's Creative Commons licence, unless indicated otherwise in a credit line to the material. If material is not included in the article's Creative Commons licence and your intended use is not permitted by statutory regulation or exceeds the permitted use, you will need to obtain permission directly from the copyright holder. To view a copy of this licence, visit <http://creativecommons.org/licenses/by/4.0/>.

© The Author(s) 2024